Design of Cylindrical Dielectric Resonators in Inhomogeneous Media

RENÉ R. BONETTI AND ALI E. ATIA, MEMBER, IEEE

Abstract—**An iterative analytical method is presented for computing resonant frequencies of dielectric cylindrical resonators in inhomogeneous media. Normalized design charts are presented including a wide range of practical geometrical and physical parameters. Numerical results, when compared to three independent sets of experimental data, show an accuracy of better than 1 percent.**

I. Introduction

INTEREST in the utilization of high-dielectric-constant resonators has been revived recently because of the availability of low-loss temperature-stable materials [1], [2]. Among the many possible applications of these resonators are temperature-compensated oscillators [3], [4], low-noise microwave synthesizers [5], and narrow-bandpass filters [6].

Several approximate methods have been presented for determining the resonant frequency of a dielectric cylinder in the presence of either one [7] or two [8] conductor planes perpendicular to its axis. In practice, when a resonator is used in a microwave circuit employing a microstrip transmission medium, the microstrip substrate as well as other dielectric supports and metallic boundaries can significantly alter the resonant frequency predicted from the idealized conditions usually assumed.

This paper describes an accurate analytical method to compute the resonant frequency of a high-dielectric-constant cylinder inside a metallic cylindrical cavity, which includes a microstrip dielectric support and several options for supporting the resonator (Fig. 1). The basic assumptions are as follows.

a) All dielectric materials involved are isotropic and lossless.

b) The metallic boundaries are perfectly conducting.

c) The electromagnetic field distribution is that of the dominant $TE_{10\delta}$ mode. (The subscripts refer to the cylindrical coordinates r, θ, and z, respectively.)

II. Method of Analysis

Fig. 2 shows the configuration to be analyzed, which consists of a cylindrical high-dielectric-constant material (region 3) positioned between three layers of different dielectrics (regions 1, 2, and 4). The $TE_{10\delta}$-mode field components in the ith region can be written as [9]

Manuscript revised December 1, 1980. This paper is based upon work performed at COMSAT Laboratories under the sponsorship of the International Telecommunications Satellite Organization (INTELSAT). A condensed version of this paper was presented at the 1980 IEEE-MTT International Microwave Symposium, Washington, DC.

The authors are with COMSAT Laboratories, Clarksburg, MD 20734.

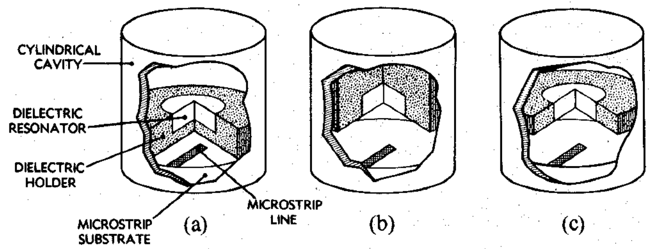

Fig. 1. Three possible ways for supporting a dielectric resonator coupled to a microstrip line. (a) From below. (b) From above. (c) From the side edge.

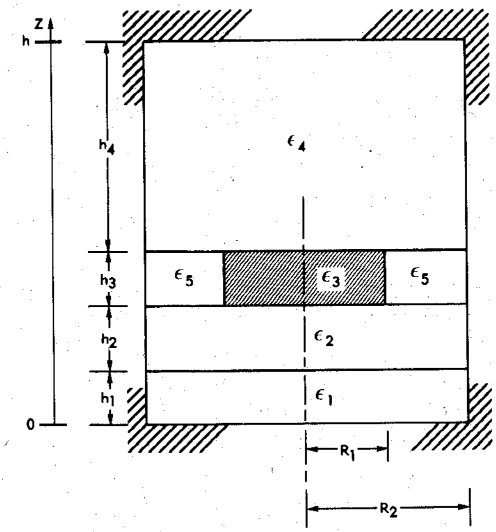

Fig. 2. Cross section of cavity under analysis.

$$H_z^{(i)} = C_0(k_i r) g_i(z) \tag{1}$$

$$H_r^{(i)} = \frac{1}{k_i} C_0'(k_i r) g_i'(z) \tag{2}$$

$$E_\phi^{(i)} = \frac{j\omega\mu_0}{k_i} C_0'(k_i r) g_i(z) \tag{3}$$

$$H_\phi^{(i)} = E_r^{(i)} = E_z^{(i)} = 0 \tag{4}$$

with

$$C_0(k_i r) = J_0(k_i r), \qquad r \leq R_1$$

$$C_0(k_i r) = K_0(k_i r) - \frac{K_0'[k_i R_2] I_0(k_i r)}{I_0'[k_i R_2)]}, \qquad R_1 \leq r \leq R_2$$

where J_0, K_0, and I_0 are the appropriate Bessel functions that describe the field distribution in the cylindrical region $r \leq R_1$ and the radially decaying fields for $r > R_1$. Also

$$g_i(z) = A_i \sinh \zeta_i z + B_i \cosh \zeta_i z, \qquad i=1,2,4 \tag{5a}$$

$$g_i(z) = A_i \sin \zeta_i z + B_i \cos \zeta_i z, \qquad i=3,5. \tag{5b}$$

The radial and axial wavenumbers (k_i and ζ_i) are related by the wave equation as

$$k_i^2 = \omega^2 \mu_0 \epsilon_i \pm \zeta_i^2 \tag{6}$$

where the minus sign holds for $i=3$ and 5. The field decay in the radial direction for $r > R_1$ implies that the wavenumber

$$(jk_5)^2 = \zeta_5^2 - \omega^2 \mu_0 \epsilon_5 \tag{7}$$

is a real number. This condition will hold only when ϵ_5 is small as compared to ϵ_3.

Of the ten unknown constants (A_i's and B_i's) in (1)–(4) for the field components, eight are related by the boundary conditions

$$E_\phi^{(i)}(r,z) = 0, \qquad i=1,4, \quad z=0,h \tag{8}$$

$$\frac{d^m E_\phi^{(1)}(r,h_1)}{dz^m} = \frac{d^m E_\phi^{(2)}(r,h_1)}{dz^m} \tag{9}$$

$$\frac{d^m E_\phi^{(2)}(r,h_1+h_2)}{dz^m} = \frac{d^m E_\phi^{(3)}(r,h_1+h_2)}{dz^m} \tag{10}$$

$$\frac{d^m E_\phi^{(3)}(r,h_1+h_2+h_3)}{dz^m} = \frac{d^m E_\phi^{(4)}(r,h_1+h_2+h_3)}{dz^m} \tag{11}$$

with $m=0,1$, totaling a set of eight linear equations. The existence of nonzero solutions for the above system implies that

$$\frac{\zeta_3/\zeta_4 \tanh\theta_4 \tan\theta_3 - 1}{\zeta_3/\zeta_4 \tanh\theta_4 + \tan\theta_3} + \frac{p\zeta_3/\zeta_2 \tan\theta_3 - 1}{p\zeta_3/\zeta_2 + \tan\theta_3} = 0 \tag{12}$$

where

$$p = \frac{\zeta_2/\zeta_1 \tanh\theta_1 + \tanh\theta_2}{1 + \zeta_2/\zeta_1 \tanh\theta_1 \tanh\theta_2}$$

$$\theta_i = \zeta_i h_i, \qquad i=1,\cdots,4.$$

The relationship between the ζ_i follows from

$$k_1 = k_2 = k_3 = k_4 \tag{13}$$

$$\zeta_5 = \zeta_3. \tag{14}$$

Since

$$\zeta_3 = \frac{\delta\pi}{h_3}$$

where δ defines the mode, (6) and (13) yield

$$\theta_i = \left[\omega^2 \mu_0(\epsilon_3 - \epsilon_i) - \left(\frac{\delta\pi}{h_3}\right)^2\right]^{1/2} h_i, \qquad i=1,2,4. \tag{15}$$

Equation (12), therefore, has two unknowns, δ and ω. Another equation follows from the continuity of the fields, which at the resonator's edge can be written in terms of the wall admittance matching

$$\vec{Y} + \overleftarrow{Y} = 0 \tag{16}$$

where

$$\vec{Y} = \left.\frac{H_z^{(5)}}{E_\phi^{(5)}}\right|_{r=R_1}, \qquad \overleftarrow{Y} = -\left.\frac{H_z^{(3)}}{E_\phi^{(3)}}\right|_{r=R_1}.$$

Equation (16), together with (1)–(3), yields

$$k_3 \frac{J_0(k_3R_1)}{J_0'(k_3R_1)} + jk_5 \frac{C_0(jk_5R_1)}{C_0'(jk_5R_1)} = 0. \tag{17}$$

A natural way of solving the system [(12) and (17)] is to iteratively start with the solution of (17) using an assumed value between 0 and 1 for δ (e.g., $\delta=0.5$), and continue by correcting this value from the solution of (12) and the value of the resonant frequency from (17). This technique can be easily implemented even on a small computer. However, the number of iterations necessary to converge to a stationary result strongly depends on the starting value. The computations presented in this paper required no more than six iterations, when the starting frequency was taken as

$$f_0 = \frac{1.2}{\pi\sqrt{\mu_0\epsilon_3}\, R_1}$$

computed via the first root of

$$J_0(k_3R_1) = 0 \tag{18}$$

with ($\delta=0$) only. It should be noted that when $h_3 \ll \lambda_0/\sqrt{\epsilon_5}$ and $R_2 \gg R_1$, the second term in (17) approaches zero and the equation becomes equivalent to (18), which corresponds to a magnetic wall boundary condition at $r=R_1$.

III. Numerical Results

The pair of eigenvalue equations, (12) and (17), can be solved in a universal form, independent of the absolute values of the parameters involved, if the following normalizations are introduced:

$$\hat{\epsilon}_i = \frac{\epsilon_i}{\epsilon_3}, \quad \hat{h}_i = \frac{h_i}{h_3}, \qquad i=1,2,4,5$$

$$\hat{R}_1 = \frac{R_1}{h_3}, \quad \hat{R}_2 = \frac{R_2}{R_1}.$$

Equation (15) can then be rewritten as

$$\theta_i = \left[\left(\frac{\hat{\omega}}{\hat{R}_1}\right)^2 (1-\hat{\epsilon}_i) - (\delta\pi)^2\right]^{1/2} \hat{h}_i \tag{19}$$

in which

$$\hat{\omega} = \omega\sqrt{\mu_0\epsilon_3}\, R_1.$$

The arguments of the Bessel function in (17) becomes

$$k_3R_1 = \left[\hat{\omega}^2 - (\delta\pi\hat{R}_1)^2\right]^{1/2} \tag{20}$$

$$jk_5R_1 = \left[(\delta\pi\hat{R}_1)^2 - \hat{\omega}^2\hat{\epsilon}_5\right]^{1/2}. \tag{21}$$

The resonant normalized frequency $\hat{\omega}$ of the dielectric resonator placed in free space can be computed from (12) and (15) with $\hat{h}_1=0$, $\hat{h}_2=\hat{h}_4\to\infty$; $\epsilon_i=\epsilon_0$ ($i=1,2,4,5$); and $R_2/R_1\to\infty$. Under these conditions, (12) and (17) become

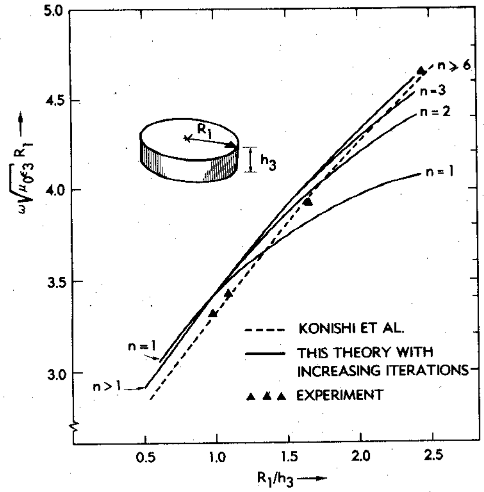

Fig. 3. Normalized resonant frequency of a cylindrical dielectric resonator in free space for an increasing number of iterations compared to the theoretical and experimental results of [9].

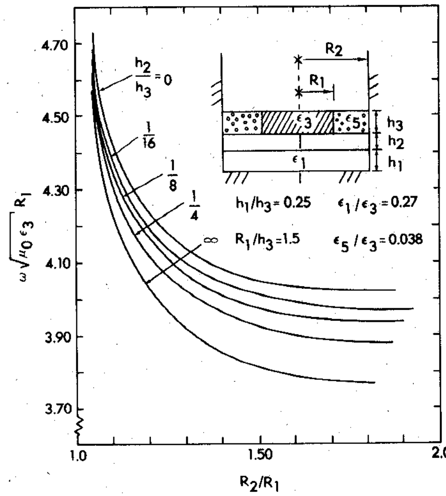

Fig. 5. Normalized resonant frequency as affected by the sidewalls.

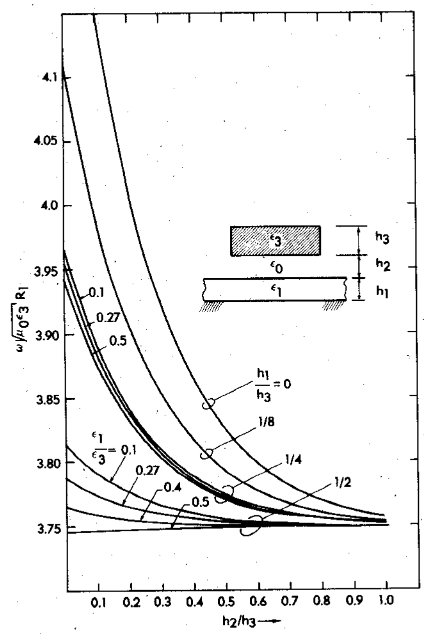

Fig. 4. Normalized resonant frequency of a dielectric disk in the presence of a dielectric-coated conductor plane.

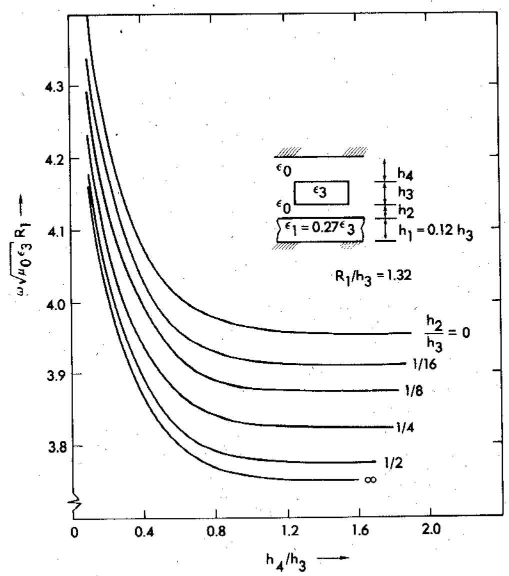

Fig. 6. Normalized resonant frequency dependence on the proximity of two conductor planes (one supporting a microstrip substrate).

$$\tan(\delta\pi) = \frac{\zeta_2}{\zeta_3} \tag{22}$$

$$k_3 \frac{J_0(k_3 R_1)}{J_0'(k_5 R_1)} + jk_5 \frac{K_0(jk_5 R_1)}{K_0'(jk_5 R_1)} = 0 \tag{23}$$

which are the same equations derived by Itoh and Rudokas [7] for this particular case.

Fig. 3 compares the convergence of the method discussed in this paper with the theoretical and experimental results of Konishi *et al.* [10]. The small error between these two approaches is that open resonators couple energy into free space; therefore, the analysis must include radiation modes. As pointed out by Itoh [7], this error decreases for higher dielectric constants. However, radiation effects are not present in closed structures, as will be exemplified in the next section.

Fig. 4 shows the effects of the proximity of a microstrip substrate on free-space resonance ($\hat{h}_{2,4} \to \infty$) for four different substrate thicknesses and a normalized dielectric constant between 0.1 and 0.5. It should be noted that the slope of these curves can be controlled by adjusting either the substrate thickness or its dielectric constant; however, for thin substrates ($\hat{h}_2 < 1/4$), a variation of 500 percent in its dielectric constant will cause less than 5-percent variation on the resonant frequency.

Fig. 5 exemplifies the dependence on the cavity radius for a dielectric resonator placed at several different positions from the substrate. It shows that the side boundaries must be placed at a minimum distance from the resonator of one and a half times its radius if they are not accounted for in the analysis. (This ratio holds for the set of parameters depicted in the insert.)

Fig. 6 gives an idea of the tunability range of a resonator

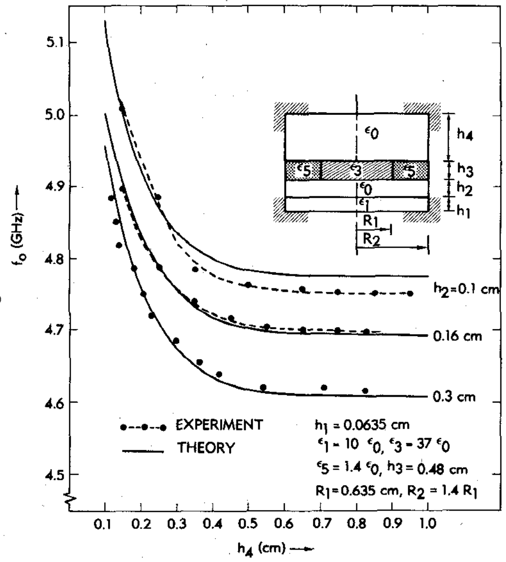

Fig. 7. Theoretical and experimental results for a prototype cavity as depicted in the insert.

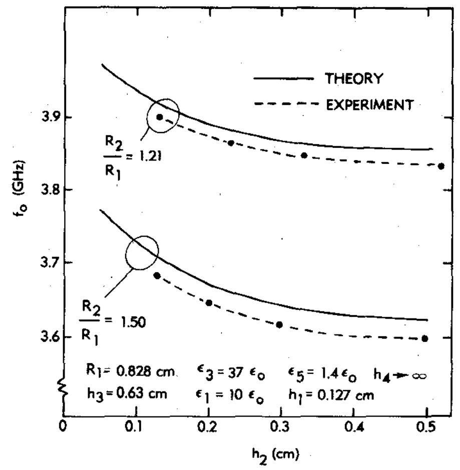

Fig. 8. Theoretical and experimental results for two different external radii.

enclosed in a flat box in which the sidewalls satisfy the condition specified above, and is useful for the design of tunable oscillators and filters. The normalized substrate dielectric constant ($\hat{\epsilon}_1 = 0.27$) corresponds, for example, to an alumina substrate ($\epsilon_1 \cong 10$) and a barium tetratitanate resonator ($\epsilon_3 \cong 37$). The ratio $R_1/h_3 = 1.32$ is close to some standard, commercially available sizes.

IV. Experimental Results

Three sets of experimental data were taken with two samples of barium tetratitanate placed within different cavities and dielectric boundaries. In the first two sets (Figs. 7 and 8) the theoretical data were computed assuming 37.0 for the resonator's dielectric constant, as measured by an independent method. The maximum error was of the order of 0.6 percent in both cases. In the third experiment, one of the theoretical curves was fitted to the experimental data to find the dielectric constant of the sample, and the result was 36.8. With this value in theoretical computations, the remaining curves show an error of 0.2 percent (Fig. 9).

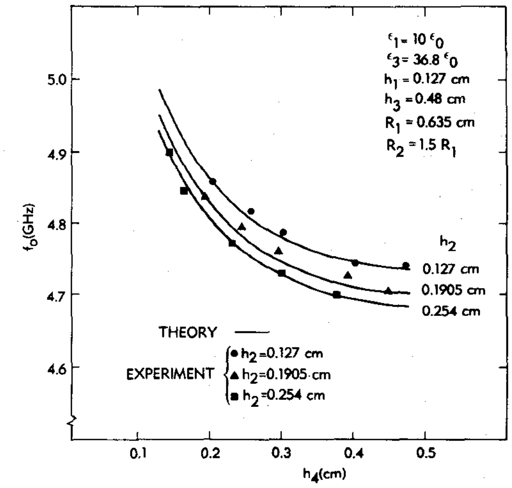

Fig. 9. Experimental results compared to theoretical computations with a dielectric constant of 36.8 (obtained from curve fitting the data set of $h_2 = 0.254$ cm).

V. Conclusions

A very accurate method was developed to compute the frequency of a cylindrical high-dielectric-constant resonator placed inside a metallic cylindrical cavity containing all necessary dielectric supports for both the resonator and microstrip lines. Normalized design charts have been presented, covering a wide range of the more relevant parameters.

For a resonator in free space, this method yields the same analytical expressions derived previously [7]. When compared to three independent sets of experimental data, the method shows an accuracy of better than 1 percent in all cases.

References

[1] W. Wakino *et al.*, "Microwave bandpass filters containing dielectric resonators with improved temperature stability and spurious response," in *Proc. 1975 Int. Microwave Symp.*, pp. 63–65, May 1975.

[2] J. K. Plourde *et al.*, "Ba_2TigO_2 as a microwave dielectric resonator," *J. Amer. Ceramic Soc.*, vol. 58, no. 9–10, pp. 418–420, 1975.

[3] ____, "A dielectric resonator oscillator with 5 ppm long term frequency stability at 4 GHz," in *IEEE MTT-S Int. Microwave Symp. Dig.*, pp. 273–276, June 1977.

[4] S. Tatsuguchi *et al.*, "An integrated 18 GHz receiver front end using a dielectric resonator stabilized generator," in *ICC 79, Conf. Rec.*, vol. 2, pp. 26.2.1–5.

[5] G. D. Alley and H. C. Wang, "An ultra low noise microwave synthesizer," in *Dig. 1979 Int. Microwave Symp.* (Orlando, FL), pp. 147–149.

[6] J. K. Plourde and D. F. Linn, "Microwave dielectric resonator filters utilizing $BA_2TI_2O_{20}$ ceramics," in *Dig. 1977 Int. Microwave Symp.* (San Diego, CA), pp. 290–293.

[7] T. Itoh and R. Rudokas, "New method for computing the resonant frequency of dielectric resonators," *IEEE Trans. Microwave Theory Tech.*, vol. MTT-25, pp. 52–54, Jan. 1977.

[8] M. Jaworski and M. W. Pospieszalski, "An accurate solution of the cylindrical dielectric resonators problem," *IEEE Trans. Microwave Theory Tech.*, vol. MTT-27, pp. 639–642, July 1979.

[9] J. C. Sethares and S. J. Naumann, "Design of microwave dielectric resonators," *IEEE Trans. Microwave Theory Tech.*, vol. MTT-14, pp. 2–7, Jan. 1966.

[10] Y. Koniski, N. Hoshino, and Y. Utsum, "Resonant frequency of a $TE_{01\delta}$ dielectric resonator," *IEEE Trans. Microwave Theory Tech.*, vol. MTT-24, pp. 112–114, Feb. 1976.